FOREST-AIR FLUXES OF CARBON, WATER AND ENERGY OVER NON-FLAT TERRAIN

XUHUI LEE* and XINZHANG HU
School of Forestry and Environmental Studies, Yale University, 370 Prospect Street, New Haven, Connecticut 06511, USA

(Received in final form 12 October 2001)

Abstract. A field study of surface-air exchange of carbon, water, and energy was conducted at a mid-latitude, mixed forest on non-flat terrain to investigate how to best interpret biological signals from the eddy flux data that may be subject to advective influences. It is shown that during periods of Southwest winds (sector with mild topography), the eddy fluxes are well-behaved in terms of energy balance closure, the existence of a constant flux layer, consistency with chamber observations and the expected abiotic controls on the fluxes. Advective influences are evident during periods with wind from a steep (15%) slope to the Northeast of the tower. These influences appear more severe on CO_2 flux, particularly in stable air, than on the energy fluxes. Large positive flux of CO_2 ($>$ 23 μmol m^{-2} s^{-1}) occurs frequently at night. The annual sum of the carbon flux is positive, but the issue about whether the forest is a source of atmospheric carbon remains inconclusive.

Attempts are made to assess vertical advection using the data collected on a single tower. Over the Southwest sector, vertical advection makes a statistically significant but small contribution to the 30-min energy imbalance and CO_2 flux variations. Contributions by horizontal advection may be larger but cannot be verified directly by the current experimental method.

Keywords: Advection, Carbon cycle, Eddy covariance, Energy balance, Evaporation, Mixed forest, Rolling topography.

1. Introduction

One goal of micrometeorological studies of vegetation-air exchange is to quantify the surface source strength by in-situ measurement of air turbulence and concentrations of the scalar of interest. This is often achieved by a 1-dimensional approximation to the surface-layer mass/energy balance: the surface flux is approximated by the sum of two easily-measured quantities, vertical eddy flux and air storage, on a single tower. In this 1-dimensional (1D) framework, all atmospheric quantities are assumed to vary only in the vertical direction. The stringent requirement this imposes on where the tower should be placed precludes studies of some biome types (e.g., alpine). In non-ideal or more realistic conditions (tall vegetation, non-flat terrain, patchy canopy, free convection, rain, stable stratification), the flow within and above the canopy can become 2- or 3-dimensional, leading to advection that the conventional tower instruments are unable to capture. Philip (1959)

* E-mail: xuhui.lee@yale.edu

Boundary-Layer Meteorology **103:** 277–301, 2002.

stated, 'The possibility of advection has been recognized mainly in a negative way. Experimenters attempt to avoid it by working downstream of extensive "homogeneous" area. Sometimes advection is invoked to explain otherwise inexplicable observations'. His statement is equally valid now as it was 40 years ago.

Currently there are over 100 research groups within the FluxNet network that deploy the above 1D methodology on a continuous basis to investigate energy, water and carbon fluxes between various types of vegetation and the atmosphere (Baldocchi et al., 2001). A large number of the sites are on non-flat terrain. A question common to the non-flat sites is how to best interpret biological signals from data that is prone to advective influences. Motivated in part by the need to address this question, we conducted a field experiment on energy and carbon exchanges in a mixed forest on rolling terrain. The objectives of this paper are (a) to investigate the degree to which advection can be related to topography and air stability, and the relative roles of vertical and horizontal advection, and (b) to determine whether advection exerts an equal influence on fluxes of sensible heat, water vapour and carbon dioxide. Our strategy is to use those aspects of the forest-air exchange, such as energy balance, constant flux layer, response of carbon flux to light, that have been established in ideal conditions, as benchmarks to judge the degree of advective influence. Of special interest is how data obtained on a single tower can be used to gain insight into the advection problem. Our experimental design also offers an opportunity of assessing tower interference with the flux measurement; this is summarized in Appendix A.

2. Theoretical Considerations

2.1. Mass conservation

At the outset of the analysis, it is useful to present the mass conservation equation and comment briefly on various assumptions and simplifications needed to interpret biophysical meanings of the tower flux data. The usual symbol convention is adopted here by which t is time, prime denotes departure from the mean, overbar is the Reynolds averaging operator, and u and w are velocity components in the x (longitudinal) and z (normal to terrain surface) directions, respectively. Integration of the 2D mass conservation equation for a scalar, q, and the continuity equation with respect to z gives the following

$$(\overline{w'q'})_r + \int_0^{z_r} \frac{\partial \overline{q}}{\partial t}\,\mathrm{d}z = \mathrm{NEE}_L - \int_0^{z_r} \overline{u}\frac{\partial \overline{q}}{\partial x}\,\mathrm{d}z - \overline{w}_r \Delta_q, \tag{1}$$

where $\Delta_q = \overline{q}_r - \frac{1}{z_r}\int_0^{z_r} \overline{q}\mathrm{d}z$, subscript r denotes values at the measurement height z_r, and NEE_L, termed *local* net ecosystem exchange (NEE) with the atmosphere, is defined as

$$\mathrm{NEE}_L = (\overline{w'q'})_0 + \int_0^h s\mathrm{d}z, \tag{2}$$

where h ($< z_r$) is canopy height, s is source strength, and subscript 0 denotes values at the ground level. The above vertical integration is performed at the tower location, with the assumption that $\overline{w}$ is proportional to z. (A thorough discussion of this assumption is given by Finnigan, 1999.) Also the reader is reminded that divergence of the horizontal flux is assumed negligible

$$\frac{\partial \overline{u'q'}}{\partial x} = 0. \tag{3}$$

A few general comments can be made on Equation (1). The sum of the terms on LHS of Equation (1), eddy flux and air storage, which are easily measured on a single tower, is identical to NEE_L in the absence of horizontal (term 2, RHS of Equation (1)) and vertical advection (term 3, RHS), or in situations of perfect horizontal homogeneity in both the flow and source strength. The influence of flow inhomogeneity ($\overline{w} \neq 0$) on the flux observation is a subject of recent, active debates (Lee, 1998; Finnigan, 1999; Baldocchi et al., 2000; Paw U et al., 2000). Studies of horizontal advection, on the other hand, have a long history (e.g., Philip, 1959; Garratt, 1990). These studies usually invoke the simplification that the turbulent flow field is horizontally homogeneous (i.e., $\overline{w} = 0$, etc.) and hence nonzero horizontal (passive) scalar gradients arise only from a source strength distribution that is not uniform in the streamwise direction. Horizontal advection, except in a limited number of studies (Lang et al., 1974; Rider et al., 1963), is not determined experimentally, because of the difficulty in measuring the extremely small horizontal gradient, $\partial\overline{q}/\partial x$. Some qualitative understanding can be advanced if we consider horizontal advection as a contribution to the eddy flux by the upwind source within the flux footprint (e.g., Horst and Weil, 1992; Schmid, 1994). With this view in mind, one can consider

$$[\mathrm{NEE}] = \mathrm{NEE}_L - \int_0^{z_r} \overline{u}\frac{\partial \overline{q}}{\partial x}\mathrm{d}z.$$

as a footprint adjusted NEE of some sort. For example, a negative $\partial\overline{q}/\partial x$ will develop if the source upwind of the tower is stronger than that near the tower, and therefore the vertical eddy flux, corrected for the air storage, will exceed the local NEE. This interpretation is of interest because it may make it possible to assess horizontal advection with footprint theory, hopefully requiring a single tower only. However, a quantitative footprint interpretation of horizontal advection will have

to overcome two limitations of the existing footprint models. First, the diffusion principle underlying these models is developed for the surface layer with a small surface roughness, not for the surface layer over tall vegetation. Second, these models are most accurate at near-neutral stabilities. In 'low flux events' in very stable air, a nonzero horizontal gradient may arise even for a horizontally homogeneous flow field and a uniform source strength. Mathematically, this is achieved by choosing, in Equation (1),

$$(\overline{w'q'})_r = \overline{w}_r = \partial\overline{q}/\partial t = 0. \tag{4}$$

In this extreme case, the only thing that can balance the local NEE is the concentration gradient.

2.2. Energy balance

Measurements of net radiation flux, R_n, soil heat flux, G, and biomass heat storage, S_b, are usually made in a very small area, giving essentially the local values of these quantities. Energy should be in balance if the local values of sensible heat flux, H_L, and latent heat flux, λE_L, defined in the same manner as NEE_L above (Equation (2)), are quantified. The local energy balance equation is

$$R_n - S_b - G = H_L + \lambda E_L. \tag{5}$$

In reality, however, only eddy fluxes of sensible and latent heat instead of H_L and λE_L are measured. Applying Equation (1) to these fluxes, Equation (5) becomes

$$R_n - S - G = \rho c_p(\overline{w'T'})_r + \lambda(\overline{w'\rho_v})_r + \int_0^{z_r} \overline{u}\frac{\partial J}{\partial x}\mathrm{d}z + \overline{w}_r\Delta_J, \tag{6}$$

where S is the total heat storage (including S_b) below height z_r, ρ is air density, c_p is specific heat of air at constant pressure, λ is latent heat of vaporization, T is potential temperature, ρ_v is water vapour density, $J = \rho c_p\overline{T} + \lambda\overline{\rho}_v$, and $\Delta_J = J_r - \dfrac{1}{z_r}\displaystyle\int_0^{z_r} J\,\mathrm{d}z$.

Energy imbalance is given as

$$\begin{aligned} I &= R_n - S - G - \rho c_p(\overline{w'T'})_r - \lambda(\overline{w'\rho_v})_r \\ &= \int_0^{z_r} \overline{u}\frac{\partial J}{\partial x}\,\mathrm{d}z + \overline{w}_r\Delta_J \end{aligned} \tag{7}$$

Equation (7) shows that even with a perfect measurement system, energy imbalance can exist owing to a heterogeneous horizontal source distribution, flow convergence, or both.

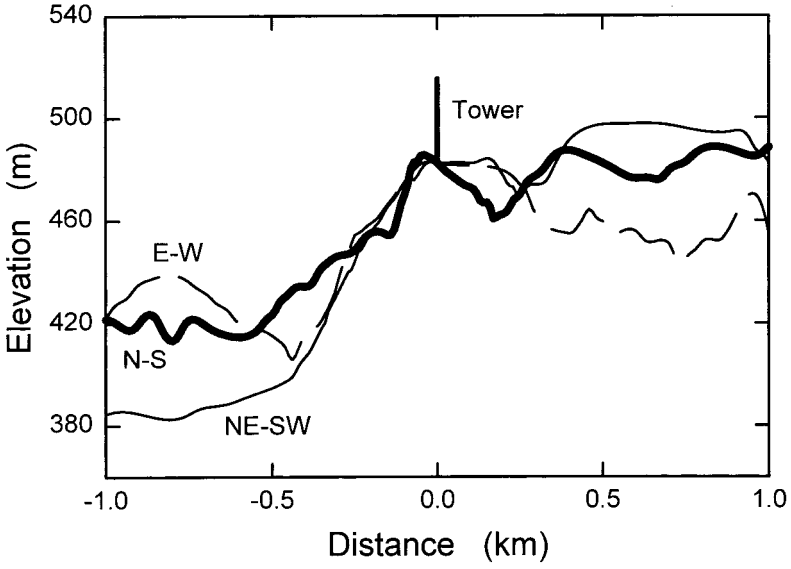

Figure 1. Three transects of terrain elevation showing the topography within 1 km of the tower.

3. Experimental Method

3.1. Site

The experimental site (41°58′ N, 73°14′ W) is in the Great Mountain Forest on moderately hilly terrain in Norfolk, Connecticut. The area within a 2-km radius of the tower is forested except for four small ponds (100–200 m wide) about 1 km to the NE, NW, SE and SW of the tower. Terrain elevation varies between 380–480 m above mean sea level (Figure 1). There is a steep slope (15%) to the northeast of the tower. In comparison, terrain variation in the SE-S-NW sector is much more mild. In order to isolate the slope effect on the fluxes, we will separate the data into two groups according to wind direction, one group with wind from 300°–120° and the other with wind from 120°–300° which are labeled as NE and SW sectors, respectively, for convenience of presentation.

The forest is a mixture of stands of natural regeneration and plantation (Winer, 1955; age 60–120 years). Tree height varied between 16–22 m; this variation smooths out the terrain roughness somewhat because tall trees are found in depressions. The main tree species in the dominant wind sector were red maple (18% basal area), eastern white pine (17%), and hemlock (21%). Leaf area index, measured with an LAI meter (model Licor-2000, LI-Cor, Inc., Lincohn, NE), was 4.1 near the tower in August, 1999. The live basal area was 33 m^2 ha^{-1} and stem (> 50 mm) density was 894 stems ha^{-1}.

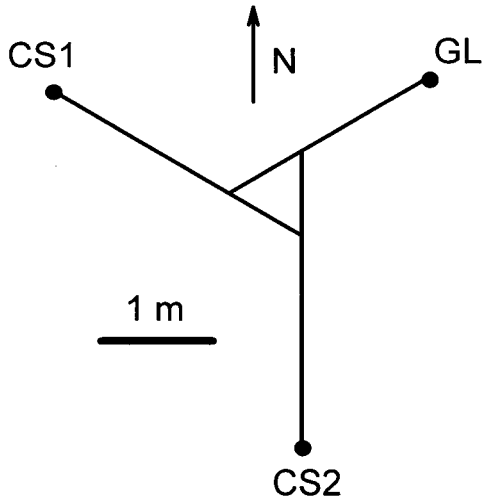

Figure 2. Arrangement of three 3D sonic anemometers/thermometers at 30.4 m above the ground, May 1999–April 2000. The face of the open lattice tower is 0.88 m wide.

3.2. INSTRUMENTATION

The experiment started in May 1999 and has continued to date since then. The analysis presented in this paper relies mostly on the data from 1999. Over the period May 1999–April 2000, three 3D sonic anemometers were operated at 30.4 m above the ground and arranged 120° apart from one another (Figure 2; CS1 and CS2, model CSAT3, Campbell Scientific, Logan, Utah; GL, model 1012R2A, Lymington, U.K.) on a triangular tower. One purpose of the redundancy was to minimize the aerodynamic shadow influence of the tower on the wind statistics (Appendix A). In May 2000, unit CS1 was lowered to the height of 21.0 m and oriented towards WSW. A krypton hygrometer (model KH2O, Campbell Scientific) and an air inlet funnel were positioned about 0.3 m behind GL. Air was drawn from the funnel through a 40-m long tubing (Dekoron, ID 6.4 mm) at a flow rate of 29 L min^{-1}. A portion of this, 6 L min^{-1}, was passed though a CO_2/H_2O analyzer (model Licor 6262, LI-COR Inc.) in a temperature-controlled building. Typical time lags were 3.8 and 4.5 s for CO_2 and H_2O, respectively. Analog signals from these instruments were first sampled by an A/D system (model PCI-6033E, National Instrument, Austin, Texas) at 120 Hz and then block-averaged to 10 Hz for analysis and archiving. In parallel to the A/D system, SDM signals from CS1 and CS2 were recorded at 5.33 Hz and the digital signal from GL was recorded at 20.8 Hz.

Air temperature was measured at nine levels (1.1, 4.7, 7.4, 11.5, 15.6, 19.1, 23.7, 27.8, 31.7 m above the ground) with fine wire thermocouples (chromel-constantan, 25 μm diameter). H_2O and CO_2 concentrations were measured at five levels (1.5, 7.4, 13.6, 21.7, 30.7 m above the ground) with a manifold system and

a gas analyzer (model Licor 6262). These profile data were used to compute the corresponding storage terms and vertical gradients of the vertical advection term (Equations (1) and (7)). Auxiliary measurements include net radiation (model S1, Swissteco, Oberriet, Switzerland), relative humidity, photosynthetic photon flux density, wind speed, wind direction, rain, and soil heat flux. The heat storage term, S, was estimated following the procedure of Lee and Black (1993).

Both the profile and eddy covariance gas analyzers were operated in absolute mode and were calibrated for zero and span once a week. The net radiometer was calibrated against a laboratory standard in May 1999 and July 2000. These two calibrations differ by less than 1%.

Over the period April–December, 2000, soil CO_2 flux was measured with a soil chamber system (Model Licor 6200, Li-Cor, Inc.) over two 50-m transects at 10 locations each. One transect extended to NE from the tower and the other to W. The measurement was made at a weekly interval.

3.3. Eddy fluxes and corrections

Our measurement system produced the above-canopy eddy fluxes of sensible heat (subscript r is dropped hereafter) $H = \rho c_p \overline{w'T'}$, latent heat, $\lambda E = \lambda \overline{w'\rho_v'}$, CO_2, $\overline{w'c'}$, and momentum, $\overline{u'w'}$, at 30-min intervals. For each 30-min period, the 3D anemometer that was least affected by the tower was selected for determining H and $\overline{u'w'}$. Data from the krypton hygrometer were not used in this analysis as its signal was severely contaminated by electrical noise.

Correction was made to $\overline{w'c'}$ for the water vapour density effect. (Note this correction should be made before any other corrections.) CO_2 and latent heat fluxes were corrected for tower interference using a wind direction and stability dependent correction factor (Appendix A), and for tube attenuation following the procedure of Goulden et al. (1997) and Hollinger et al. (1999) with system time constants of 0.25 and 0.5–0.8 s for CO_2 and H_2O, respectively.

3.4. Sensor tilt

Of the two advection terms, vertical advection can be estimated with the profile and wind data after the vertical velocity has been corrected for sensor tilt. Let $\hat{w}$ and $\hat{u}$ be the measured 30-min mean vertical and horizontal velocities, and b is a (wind direction dependent) sensor tilt factor. The 'true' mean vertical velocity was computed as a residual

$$\overline{w} = \hat{w} - b\hat{u}. \tag{8}$$

The tilt factor b is found with a regression procedure (Lee, 1998). To avoid a slight offset of the A/D card, the mean vertical velocity was computed using the SDM data from CS2 for wind sector 120–300° and the digital data from GL for wind sector 300–120°. The tilt factor of the site, given in Figure 3, is not a sinusoidal

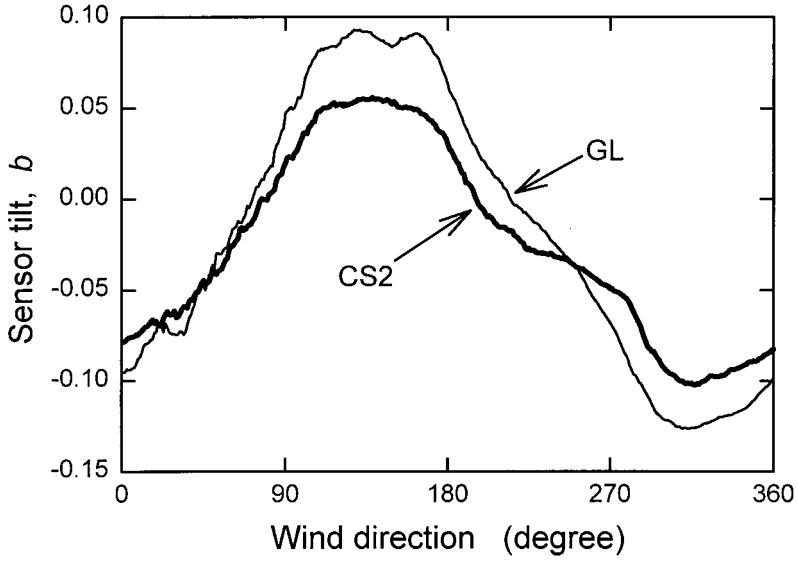

Figure 3. Sensor tilt as a function of wind direction, 1999.

function of wind direction because of the small-scale terrain variation around the tower (Figure 1).

4. Experimental Results

4.1. Mean vertical velocity

In Figure 4, the mean vertical velocity is presented for the SW sector for daytime periods. The mean vertical velocity in midday periods is positively correlated with friction velocity. (A similar trend is also found for the NW sector.) The tendency of a negative $\overline{w}$ at low friction velocity suggests that subsidence is more likely to dominate the observation than ascending motion over forests under low wind conditions. At the low u_* limit, $\overline{w}$ approaches the range of -0.04 to -0.07 m s^{-1}. At this limit, horizontal advection is small because of low wind speed, but vertical advection can be large because of large vertical gradients inside the forest in weak wind.

The nighttime $\overline{w}$ trend is less clear than in the daytime. The mean nighttime value is very small in magnitude (-0.3 mm s^{-1}) and is not significantly different from zero, suggesting that drainage flow at this site is either infrequent (Section 5.2) or is confined to a thin air layer near the forest floor.

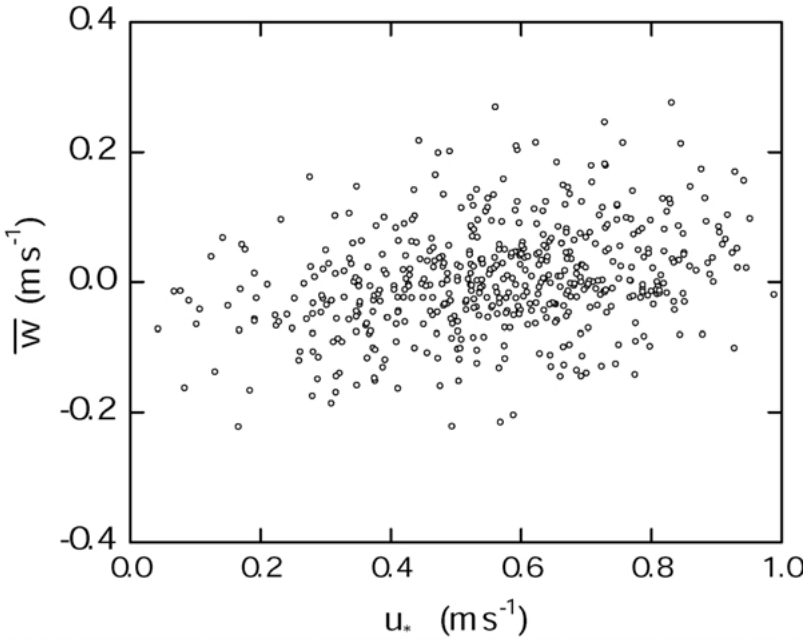

Figure 4. Mean vertical velocity ($\overline{w}$) plotted against friction velocity (u_*) for the SW sector for rainless daytime periods in June–August, 1999. A similar negative correlation is also found for the NW sector (data not shown).

4.2. Vertical flux divergence

Figure 5 presents a comparison of momentum and sensible heat fluxes measured at two heights over the canopy, after the data have been screened for the influence of the tower aerodynamic shadow and sensor biases have been removed. The fluxes appear invariant with height for the SW wind sector. Over periods of NE wind, momentum flux is 29% higher at height 30.4 m than at height 21.0 m, and the daytime sensible heat flux is 15% higher at height 30.4 m than at height 21.0 m. (The nighttime sensible heat flux over the NE wind sector differs, on average, by less than 1% between the two measurement heights.) The difference in sensible heat flux could be interpreted as an indication of source heterogeneity in the tower footprint over the NE wind sector.

4.3. Energy balance

Energy on a daily basis is closed within 7%, which is quite good in comparison with Aubinet et al. (2000) and others (Figure 6, Table I). The data are least scattered when wind comes from the mild topography (SW sector, wind direction 120–300°) and show a larger scatter when wind comes from the slope (NE sector, 300–120°) or on days of mixed wind direction. Over the NE wind sector, the sum of eddy fluxes of sensible and latent heat at height 30.4 m exceeds the available energy

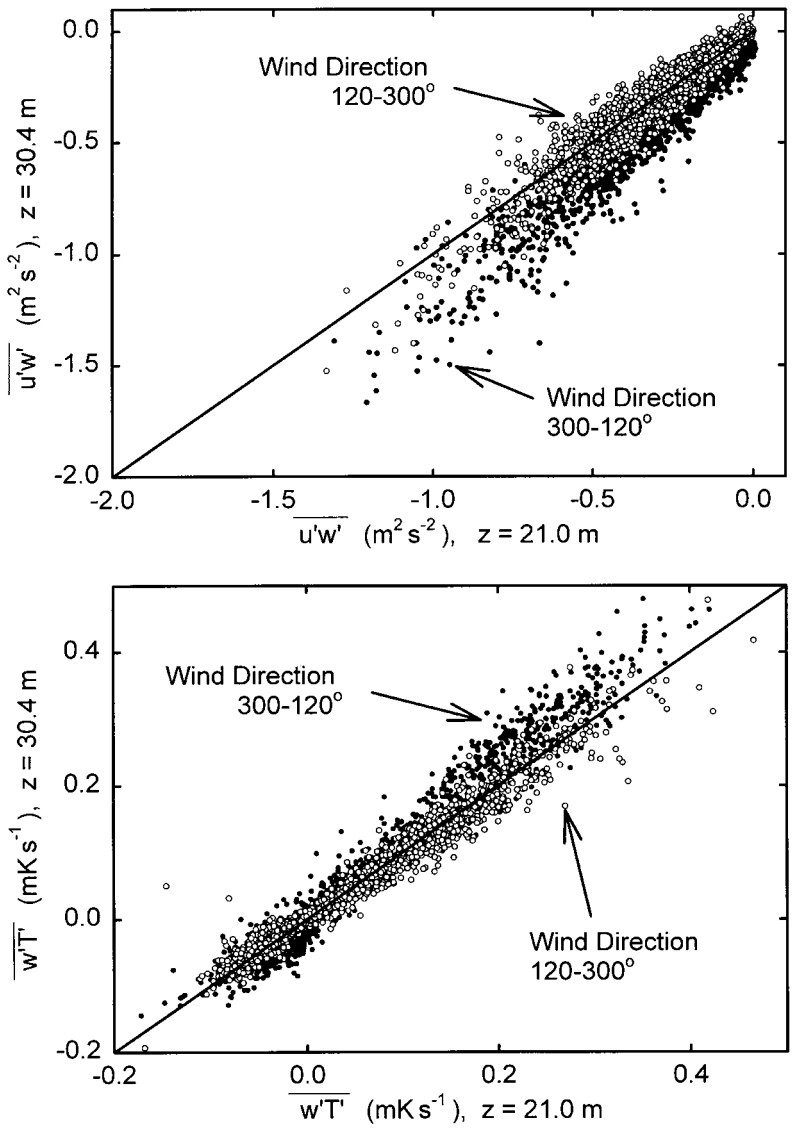

Figure 5. Vertical divergence of vertical kinematic fluxes of momentum (top) and sensible heat (bottom) over the forest, May–September, 2001 (circles, SW wind; bullets, NE wind). Also shown are 1:1 lines.

by about 7%. This is consistent with Figure 5 and is likely caused by a mismatch between the eddy flux footprint and footprint of the available energy terms. Had there been measurements of these eddy fluxes at a lower height, an even better energy balance closure would have been achieved for this wind sector. The 24-h energy balance, however, tends to mask deficiencies of the eddy covariance because the daytime energy imbalance is compensated by the nighttime energy imbalance

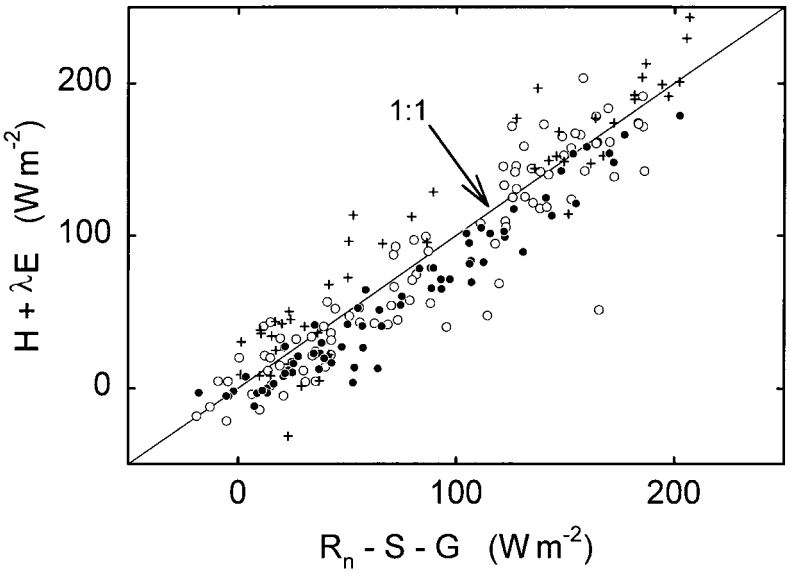

Figure 6. Daily energy balance closure by wind direction, 1999: bullets, 120–300°; crosses, 300–120°; open circles, mixed wind direction.

of opposite sign. Individual 30-min observations can suffer an energy imbalance as large as 300 W m^{-2} in magnitude.

The difficulty in closing the energy balance over short time steps is well- known. To understand the reasons for this, we have calculated the vertical advection of energy $\overline{w}\Delta_J$ (Equation (7)) using the mean vertical velocity and profile data. Figure 7 gives a comparison of the half-hourly energy imbalance, I, against the vertical advection of energy for the SW sector in the midday periods. Vertical advection explains a small but statistically significant variation of I. The remaining variation probably comes from horizontal advection and measurement errors. The aggregated measurement error can be quite large because 15 independent sensors are involved in this comparison. For the midday periods with NE wind, the correlation between I and $\overline{w}\Delta_J$ is much weaker (linear correlation 0.15, number of observations 573) than shown in Figure 7.

Correlation between I and vertical advection for the midnight periods is poor (linear correlation coefficient -0.01). This can be explained by a number of factors. First, heat storage in the biomass is a very difficult measurement. While it is a relatively small fraction over the midday periods, error in this term is comparable to other energy balance terms at night. A second factor could be that the linear assumption about $\overline{w}$ is in error (Lee, 1998). Finally, the flux footprint is extremely large under stable conditions, and hence horizontal advection could become a large factor contributing to the energy imbalance.

TABLE I

Energy balance statistics for 24-h, day (0700–1800 EDT) and night (1800–0700 EDT) periods in 1999. The linear fit is based on an orthogonal linear regression (Press et al. 1992), y is sum of eddy fluxes of sensible and latent heat ($H + \lambda E$, W m^{-2}), x is available energy ($R_n - S - G$, W m^{-2}), r is linear correlation coefficient, and n is number of observations.

Wind direction	Regression	r	n
	24-hour		
120–300°	$y = -12 + 0.96x$	0.97	67
300–120°	$y = 4 + 1.07x$	0.95	51
Mixed	$y = -9 + 1.04x$	0.93	93
	Day		
120–300°	$y = -27 + 0.92x$	0.98	83
300–120°	$y = 0 + 1.08x$	0.97	73
Mixed	$y = -28 + 1.02x$	0.96	55
	Night		
120–300°	$y = 3 + 0.87x$	0.79	101
300–120°	$y = 5 + 1.03x$	0.55	82
Mixed	$y = 5 + 0.92x$	0.29	31

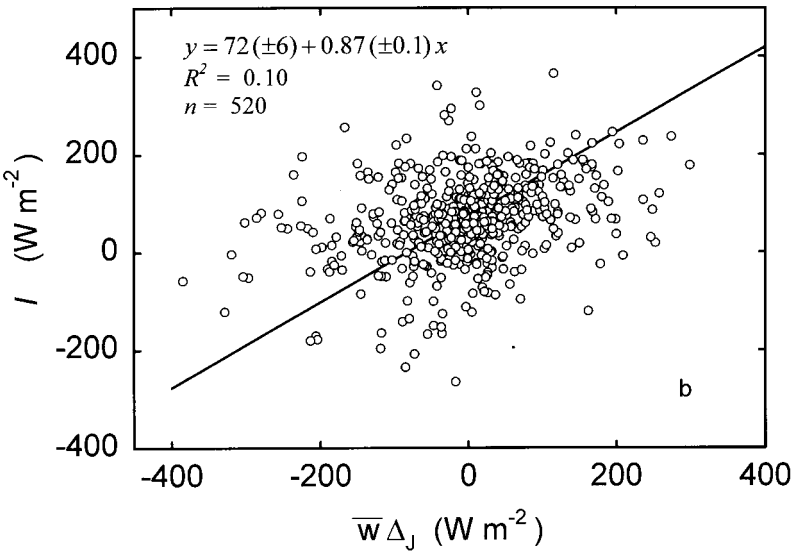

Figure 7. Scatter plot of 30-min energy imbalance versus vertical advection for daytime (1000–1600 EDT) periods with SW wind, June–August, 1999.

TABLE II

Linear correlation coefficient between CO_2 flux residual $F_c - \hat{F}_c$ and environmental variables for periods with PPFD > 800 μmol m^{-2}, June–August 1999. Here $\hat{F}_c$ is estimated with the regression equations (Figure 8). Number of observations is 500–600. Other variables are defined in the text.

Direction	I	H	λE	u_*	$\overline{w}$	$\overline{w}\Delta_C$	VPD	T_a	g_c
120–300°	0.47	−0.25	−0.25	−0.30	−0.13	−0.16	0.38	0.20	−0.50
300–120°	0.21	−0.39	−0.00	−0.09	−0.00	−0.02	0.25	0.21	−0.16

4.4. CO_2 FLUX

4.4.1. *Daytime CO_2 Flux*

CO_2 flux, F_c, corrected for the air storage term, of the forest in the SW sector shows a strong dependence on radiation (Figure 8a). The variance explained by the rectangular hyperbola model (R^2) is 70% which is typical of forests of a similar density but is lower than the R^2 values found for crops (e.g., Baldocchi et al., 1994; Rochette et al., 1995). To investigate the influence of other environmental variables on the flux, we standardize the flux by computing a flux residual ($F_c - \hat{F}_c$) (Hollinger et al., 1994), noting that the residual is negative for data below the regression line, that is, during periods of large downward flux, and vise versa. Carbon uptake seems suppressed under clear skies. Effects of vapour pressure deficit (VPD), canopy conductance (g_c) and temperature are also evident (Table II, Figure 9).

The correlation of the flux residual with vertical advection is statistically significant for the SW wind sector (Table II) but is much weaker than the correlation for the energy imbalance shown in Figure 7. This could be explained by the magnitude of the vertical gradient relative to the corresponding flux. Both the soil and vegetation are sources of heat and water vapour, resulting in a large negative Δ_J (midday ratio $\Delta_J/(H + \lambda E) \simeq -3$ s m^{-1}). On the other hand, the CO_2 gradient $\Delta_C = \overline{C}_r - \frac{1}{z_r}\int_0^{z_r} \overline{C} \mathrm{d}z$ is smaller because the soil source and foliage sink offset each other (midday $\Delta_C/F_c \simeq -0.8$ s m^{-1}).

Another point brought out by the data in Table 2 is a self-correlation among the eddy fluxes. A less negative F_c (smaller flux into the forest, or more positive flux residual) tends to occur when H, λE, or u_*, is smaller, as indicated by the negative correlation of the flux residual with these eddy fluxes. Interestingly, the correlation with energy imbalance I is much stronger than with either H or λE alone. We interpret this to suggest that the energy flux source and CO_2 sink upwind of the tower are correlated. In other words, in a footprint where there is a fast energy exchange between the vegetation and the atmosphere and presumably large

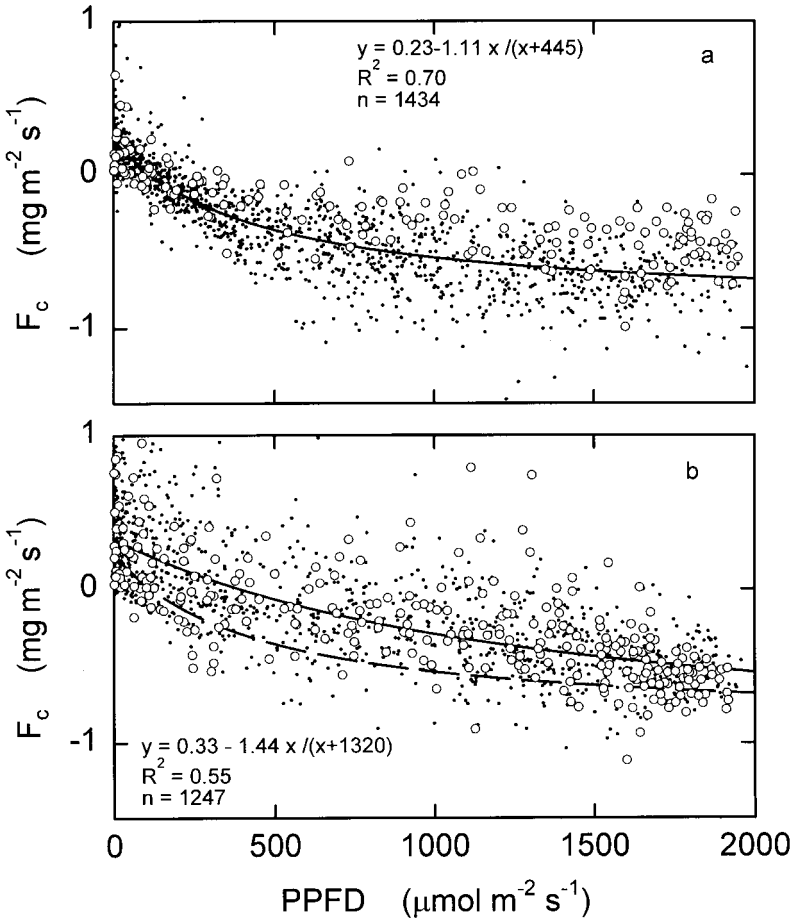

Figure 8. Response of 30-min CO_2 flux to photosynthetic photon flux density (PPFD) for SW (a) and NE wind sector (b), June-August, 1999. Observations under clear skies are shown as open circles. Also given are a model fit (line and equation), variance explained by the model (R^2) and number of observation (n). For reference, the regression fit in panel a is plotted in panel b as dashed line.

available energy, a large CO_2 uptake is to be expected. For comparison, the I versus $F_c - \hat{F}_c$ correlation is 0.32 for an even aged, homogeneous boreal forest on flat terrain documented by Black et al. (1996).

The CO_2 flux for the NE sector is more difficult to interpret than the other sector. Environmental influence becomes either less clear (PPFD, VPD, g_c) or no longer detectable (cloudiness; Figure 8b, Table II). The overall less negative flux and a large scatter imply a large contribution of the soil efflux that is insensitive to these environmental factors, or large advection due to disturbance to the flow by the terrain slope (Figure 1) or a source heterogeneity in this sector.

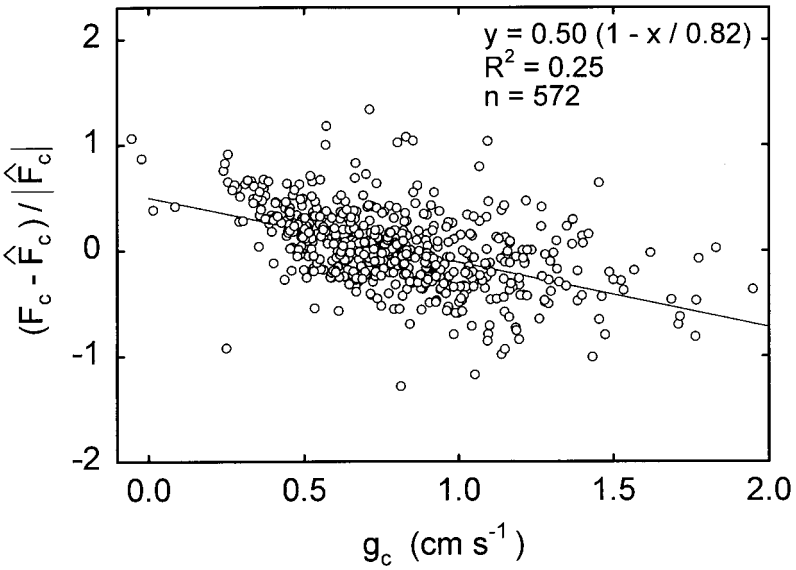

Figure 9. Normalized CO_2 flux residual, $(F_c - \hat{F}_c)/\hat{F}_c$, plotted against canopy conductance (g_c) computed with a big leaf model for periods with PPFD > 800 μmol m^{-2}, June –August, 1999.

4.4.2. *Nighttime CO_2 Flux*

Figure 10 shows a 9-day (4–12 July) time series of the eddy CO_2 flux, CO_2 gradient over the forest, CO_2 profile, and friction velocity u_*. The average 50-mm soil temperature over days 186–188 is 20.5 °C, the highest of the year, and decreases to 15.5 °C over days 192–194. Nighttime CO_2 eddy flux also displays a decreasing trend with time, but the twenty-fold change, from 1 mg m^{-2} s^{-1} on day 186 to 0.05 mg m^{-2} s^{-1} on day 193, is too large to be explained solely by the temperature change. The low eddy flux and little CO_2 buildup inside the forest on day 193 suggest drainage depletion of CO_2 under weak wind (u_* = 0.2–0.3 m s^{-1}), a common suspect for causing low flux at other forests. What is unusual about this site is the frequent occurrence of large flux at night. The value on day 186 appears to be the highest nighttime eddy flux ever reported for forests.

The high flux is not caused by malfunction of the eddy covariance as it is usually associated with a large CO_2 concentration gradient over the forest and a large buildup near the forest floor despite strong mechanical mixing (e.g., u_* = 0.4–1.2 m s^{-1} on day 186). Furthermore, examination of the raw turbulence time series and their spectra shows that the large positive correlation between CO_2 and the vertical velocity is genuine.

One possible reason for the large flux is vertical advection. A typical nighttime CO_2 gradient, Δ_C, during the growing season is -5 mg m^{-3}, which is one order of magnitude larger than the daytime value of 0.3 mg m^{-3}. Hence the nighttime measurements are more prone to advection errors. In Figure 11, we compare the flux residual $F_c - \hat{F}_c$ with vertical advection of CO_2 for the SW sector. Here $\hat{F}_c$

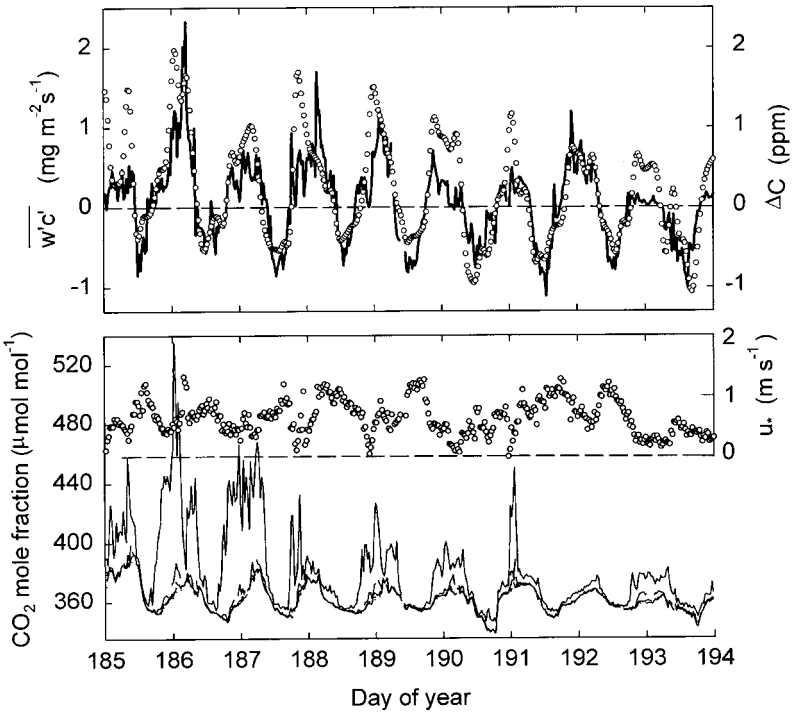

Figure 10. Top: Half-hourly eddy CO_2 flux ($\overline{w'c'}$, line) and CO_2 gradient in the air layer 21.7–30.7 m (ΔC, open circles); Bottom: CO_2 profile data (solid line, 1.5 m; data for heights of 7.4, 13.6, 21.7 and 30.7 m are indistinguishable) and friction velocity (u_*, open circles).

is computed using the regression equation against soil temperature (Figure 12). An assumption implicit in the comparison is that the regression fit can be taken as a surrogate for the local NEE of CO_2 (Equation (2)). The statistically significant correlation of $F_c - \hat{F}_c$ with $\overline{w}\Delta_C$ does suggest a (weak) role of vertical advection in the nighttime flux, particularly during times of high flux.

Separation of the data by wind direction shows a discernible pattern in the nighttime flux (Figure 12). High flux events are more frequent for the NE sector than for the SW sector. At the same soil temperature, CO_2 flux is 80% higher over the NE sector than over the SW sector. This begs the question of whether the systematic difference is biological. Large trees are abundant in the NE sector, so it is possible that the above-ground autotrophic respiration is high. Also the large CO_2 flux is usually associated with a large CO_2 buildup near the ground, for example on day 186, perhaps caused by an unidentified large soil CO_2 emission source in the NE sector. If this is true, then horizontal source heterogeneity or horizontal advection must have manifested itself as a larger-than-usual vertical concentration gradient, which, in turn, drives a large vertical eddy flux.

Another possibility is that the terrain slope to the northeast of the tower (Figure 1) produces a persistent flow convergence pattern and therefore a positive

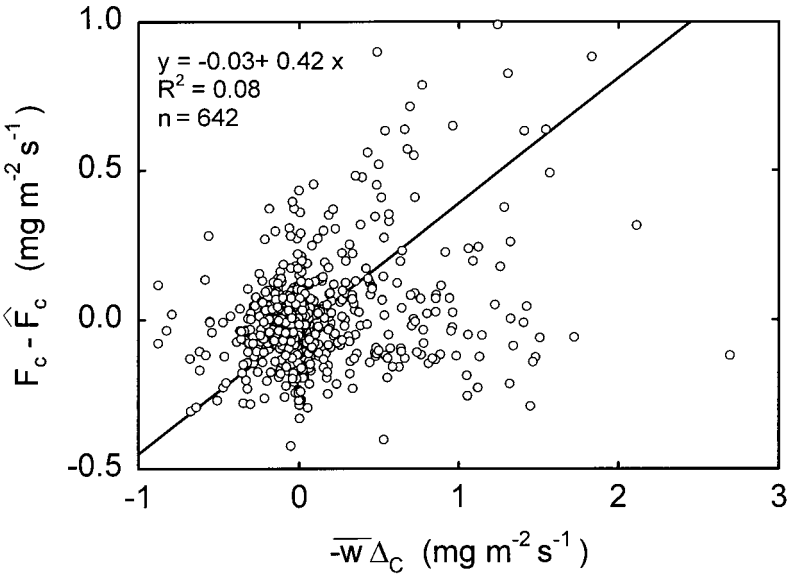

Figure 11. Comparison of CO_2 flux residual ($F_c - \hat{F}_c$) against vertical advection for the SW sector at night (22-05 EDT), June–August, 1999. Here $\hat{F}_c$ is the regression fit against soil temperature.

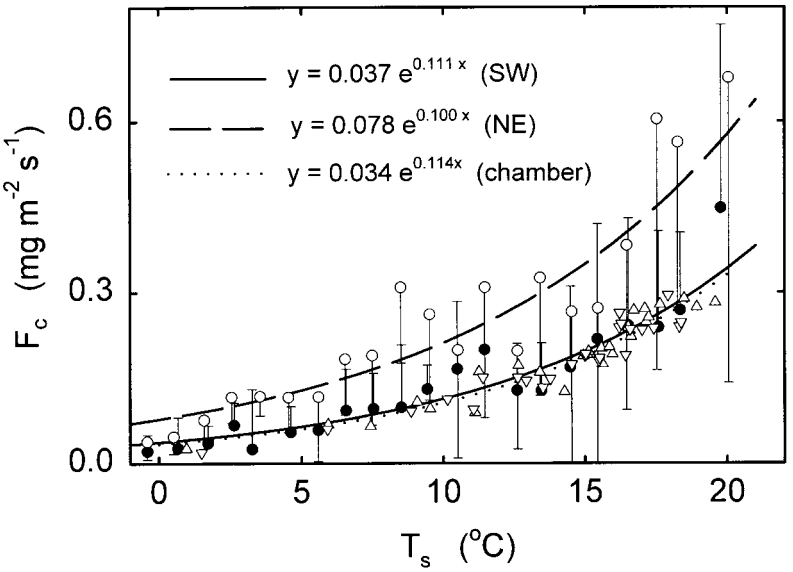

Figure 12. Nighttime (22-05 EDT) CO_2 flux as a function of 5-cm soil temperature, 1999 (open circles, NE sector; bullets, SW sector). For clarity of presentation data are averaged over 1 °C bins. Error bars are one standard deviation. Also given are measurements of soil CO_2 flux made along W (triangles) and NE (up-side-down triangles) transects in 2000.

advection flux (term 3, RHS of Equation (1), noting that Δ_C is usually negative at night), although flow convergence alone can not explain why a large CO_2 gradient develops near the forest floor and above the canopy in the first place (Figure 10). Unfortunately, a persistent flow convergence pattern cannot be detected with the above tilt correction procedure (Equation (8)).

Also given in Figure 12 is the soil chamber flux measured over two 50-m transects near the tower. Soil flux matches closely with the eddy flux observed in SW wind. Considering that soil respiration is typically 70% of the forest respiration (Goulden et al., 1997), the true whole-ecosystem respiration rate probably lies somewhere between the eddy fluxes for the two wind sectors. Regardless of the magnitude of the true biological flux, all three datasets suggest a similar rate of change in response to temperature, as indicated by the similar coefficients in the exponent of the regression equation. It seems that even imperfect fluxes can deduce reasonable biological response functions.

4.5. Seasonal variation

The sum of CO_2 flux over the period June 1999–May 2000 is +200 g C m^{-2}, with data gaps (5%) filled with the appropriate functional relationships (Lee et al., 1999) but without u_* screening of the nighttime data. The positive annual sum is in disagreement with all previous observations showing that temperate forests are sinks of carbon (Valentine et al., 2000; Schmid et al., 2000; Baldocchi et al., 2000; Lee et al., 1999; Hollinger et al., 1999; Black et al., 1996; Wofsy et al., 1993). Our annual sum should, however, be viewed with extreme caution because of the potential bias of CO_2 flux towards large positive values at night. The issue about whether this forest is a source of carbon remains inclusive.

The data presented above (Figures 5, 6 and 8, Tables I and II) indicate that the daytime fluxes of energy, water and carbon are reasonable during the mid-growing season, particularly over the SW wind sector, in comparison to those obtained over flat terrain. To further illustrate this, we have analyzed the midday CO_2 eddy flux and the daytime Priestley–Taylor parameter over a full year ending in May 2000. The seasonal variation in the midday CO_2 flux, presented in a related study (Lee et al., 2001), shows clearly that the forest shuts down photosynthesis in late November after the top soil has become frozen or nearly frozen and switches it on immediately after spring snowmelt/soil warming, consistent with findings at other flat sites (Hollinger et al., 1999; Lee et al., 1999). The Priestley–Taylor α, computed from

$$\alpha = \lambda E/[(H + \lambda E)\Delta/(\Delta + \gamma)],$$

where Δ is the slope of the saturation vapor density curve and γ is the psychrometric constant, is in the range of 0.7–1.1 during the growing season, which is at the low end of values found for forests (Wilson et al., 2000; Blanken et al., 1997; Spittlehouse, 1989) due to low surface conductance of conifers (Kelliher et

al., 1995) and limited water holding capacity of the shallow soil in our forest. The seasonal pattern of α mimics that observed at a boreal deciduous forest (Blanken et al., 1997) except that evapotranspiration does not shut down in the winter, resulting in a non-negligible α value of 0.2–0.3 even when the top soil is frozen.

5. Discussion

5.1. Source versus flow heterogeneity

In standard footprint models (e.g., Horst and Weil, 1992), horizontal advection arising from a source inhomogeneity is compensated by a change in the vertical eddy flux. Thus, a large vertical flux of CO_2 caused by horizontal advection may be indicative of the presence of a large surface source strength in the upwind footprint. In other words, micrometeorological fluxes under the influence of horizontal advection may have some biological underpinnings. In contrast, flow convergence is a property of air circulation and except for the cases noted below, is not directly dependent upon the horizontal source distribution (at least for passive scalars like CO_2). In this sense, vertical advection is a pure methodological artifact from the viewpoint of quantifying NEE with the eddy covariance.

In Equation (1), vertical advection due to flow convergence appears decoupled from the horizontal source distribution. It is understood that flow convergence is the simplest form of flow heterogeneity. If the rate of convergence is large, the surface stress will adjust to the change in wind speed, which in turn may cause a sufficiently large change in the scalar source strength. Some examples of this are discussed by Finnigan (1999) using an area integration of the mass conservation equation over the smooth-wall surface layer. In the present study, one may consider the lack of a constant flux layer for both the momentum and sensible heat fluxes over the NE wind sector as evidence suggesting such an adjustment (Figure 5). Furthermore, in an uneven forest, the source and flow heterogeneity may actually be linked. For example, the rate of forest respiration may be higher in a denser portion of the forest, while flow from a denser to a thinner portion of the forest will experience divergence in response to the density change.

5.2. Topographic effects

Uneven topography adds several elements of complexity to the observation. First, it can modify the ambient background flow through a pressure perturbation ('bluff body effect') so that the streamline may depart from the local terrain slope and the flow strictly is no longer one-dimensional (Finnigan and Brunet, 1995; Taylor et al., 1987). A consequence of this is that momentum flux is no longer constant with height according to the momentum conservation equation (Garratt, 1992; Figure 5). Second, terrain itself can generate its own thermal circulations such as nighttime gravitational or drainage flow. Finally, the source strength is usually

not horizontally homogeneous in complex terrain (e.g., Figure 5). The topographic influence is less obvious in early short-term field campaigns (e.g., Verma et al., 1986; McMillen, 1988) than in more recent long-term observations (Baldocchi et al., 2000; Lee, 1998; Finnigan, 1999; Paw U et al., 2000; Yi et al., 2000).

In a related study, Baldocchi et al. (2000) find the nighttime CO_2 flux at their ridge-top site too small in comparison with chamber observations or modelling. They attribute this largely to the influence of drainage flow. In contrast, low CO_2 flux events are less frequent at our site, occurring on average only one out of 8–10 nights during the growing season. Our data appear to indicate a stronger influence of the bluff body effect than drainage flow. One reason for this contrast is that our site is much windier: the nighttime friction velocity averaged over the growing season is 0.43 m s^{-1} at our site and only 0.15 m s^{-1} at Baldocchi's site (K. Wilson and D. Baldocchi, pers. comm., 2001). If we attribute the large CO_2 flux (>1 mg m^{-2} s^{-1}) observed at night solely to vertical advection, the mean vertical velocity would be 0.2 m s^{-1} given a typical nighttime Δ_C of -5 mg m^{-3}. The vertical velocity of this magnitude would imply a tilt of the mean streamline of 2°–5° from the local slope.

One procedure for screening nighttime flux data subject to the advective influence relies on the assumption that the biological CO_2 flux is independent of the turbulence. Unlike some less windy sites (e.g., Black et al. 1996), the nighttime CO_2 flux of this study does not show a clear roll-off against friction velocity. Interestingly, data presented by Aubinet et al. (2000) also suggest an undetectable roll-off at those EuroFlux sites with high wind.

6. Conclusions

At sites on rough topography, operationally it is useful to separate the data by wind direction. During periods of SW wind (sector with mild topography), the fluxes of energy, water and carbon dioxide are quite reasonable, in terms of energy balance closure, the existence of a constant flux layer, consistency with the chamber flux, and abiotic influences on the carbon exchange expected for a temperate forest. The well-behaved fluxes also suggest that any disturbance to the air motion by the slope in the NE sector has a minimal effect on flux observations upstream of the slope. Over half-hourly intervals, vertical advection makes a statistically significant but small contribution to the energy imbalance and CO_2 flux variations. Contributions by horizontal advection may be larger but cannot be verified directly by the current experimental method.

In comparison to the SW sector, the advective influences are much larger on the fluxes observed in NE wind, as evidenced by the lack of a constant flux layer over the canopy and the frequent occurrence of large nighttime CO_2 flux (>1 mg m^{-2} s^{-1}). Erroneous fluxes in complex terrain are not a surprise, but it is interesting to note the *magnitude* of the flux and its concurrent occurrence with a

large above-canopy concentration gradient and CO_2 buildup near the forest floor. It appears that there is an unidentified strong biological CO_2 source in this wind sector, but the magnitude of the biological signal must have been amplified by advection.

Advection does not exert an equal influence on the forest-air exchanges of energy and carbon. Eddy fluxes of water vapour and sensible heat are more robust than CO_2 flux. Even for the NE sector, the 24-h energy balance is closed to within 7%, which is quite good in comparison with Aubinet et al. (2000) and others.

Ultimately, the deviation of the micrometeorological fluxes from the true local NEE results from neglect of various terms of the mass conservation. In this study, attempts are made to assess vertical advection with the data collected on a single tower. Horizontal advection, which is by far the most difficult term to quantify, cannot be assessed directly with the current experimental setup. It is suggested that with appropriate assumptions, one may be able to infer horizontal advection from footprint models, but any attempt at a quantitative footprint interpretation of horizontal advection will have to overcome various deficiencies of the existing diffusion theory.

Acknowledgements

This work is supported by the U.S. National Science Foundation through grants ATM-9629497 and ATM-0072864, the Department of Energy NIGEC program (grant 901214-HAR), and in-kind contributions from the Great Mountain Forest Cooperation, Norfolk, Connecticut and Northeast Utilities. We also acknowledge two anonymous journal reviewers for their constructive criticisms.

Appendix A: Tower Interference with Flux and Wind Statistics

The problem of flow distortion by towers is usually investigated using the mean wind speed (Dabberdt, 1968; Clermak and Horn, 1968; Camp and Kaufman, 1970; Izumi and Barad, 1970; Moses and Daubek, 1961). Few studies have attempted to quantify the flow interference with higher-order wind statistics (Miller et al., 1999). There is little experimental data on the interference with scalar fluxes and on the effect of air stability. Here we use the data obtained with CS1 and CS2 (Figure 2) to show that flow distortion can have a substantial effect on the scalar flux, especially in stably-stratified flow.

For this analysis we select the data obtained over periods with wind direction in the range S-W-NE. In this wind direction range, CS1 is least influenced by the tower and is used as a reference, while CS2 is affected to the extent that depends on the exact wind direction (Figure A1). The aerodynamic shadow is 2–4 times as broad as the geometric shadow and is not symmetrical around the center of the

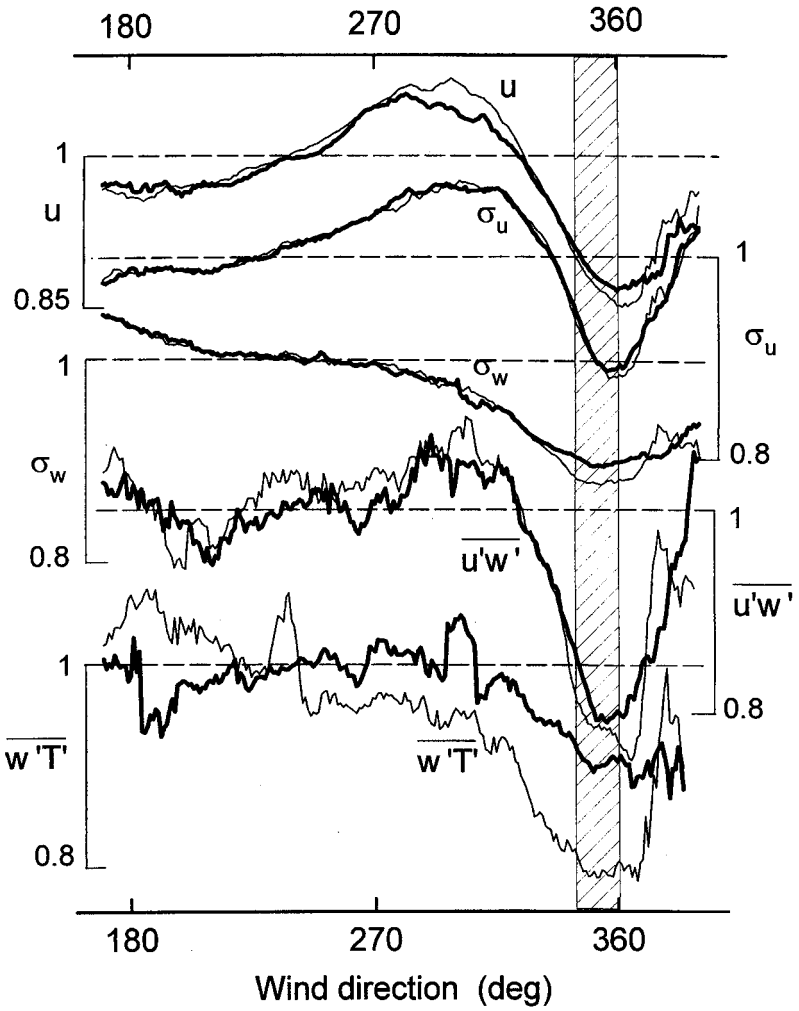

Figure A 1. Tower interference on CS2 measurement of mean wind speed (u), standard deviations of horizontal (σ_u) and vertical velocity (σ_w), momentum flux ($\overline{u'w'}$) and kinematic sensible heat flux ($\overline{w'T'}$). Thick and thin lines are for unstable and stable stratifications, respectively. All quantities are relative to the measurement with CS1. Shaded band indicates the geometric shadow of the tower as seen by CS2.

latter. Both the mean horizontal wind speed and its standard deviation shows some enhancement when wind is parallel to the tower face (roughly 300°) and reduction when wind is perpendicular to the tower face (roughly 180°). The effect of stability is small on the distortion of wind statistics but is discernible on the heat flux. The influence of flow distortion on sensible heat flux is expressed as

$$g = \begin{cases} 1 - 0.1\exp[-0.0015(\theta - \theta_c)^2] & \text{for unstable air} \\ 1 - 0.25\exp[-0.0008(\theta - \theta_c)^2] & \text{for stable air} \end{cases} \tag{A1}$$

where θ is wind direction and θ_c is the azimuth direction of the wake center. This relation is used to correct water vapour and CO_2 fluxes measured with GL assuming that the tower wake has an equal influence on all scalar fluxes.

The momentum thickness of the tower wake is given by (Tennekes and Lumley, 1972)

$$D = \int_{-\infty}^{+\infty} \frac{u}{u_o}(1 - \frac{u}{u_o})\,\mathrm{d}y,$$

where the integration is performed across the wake, and u_o is the free-stream velocity. The effective drag coefficient of the tower is given by

$$c_d = 2D/d,$$

where d (= 0.88 m) is the tower width. Using the data in Figure A1 we obtain an estimate of 0.11 m for D. The drag coefficient is then 0.25, or 1/4 of that of a circular cylinder.

References

Aubinet, M., Grelle, A., Ibrom, A., Rannik, Ü., Moncrieff, J. Foken, T., Kowalski, A. S., Martin, P. H., Berbigier, B., Bernhofer, CH., Clement, R., Elbers, J., Granier, A., Grünwald, T., Morgenstern, K., Pilegaard, K., Rebmann, C., Snijders, W., Valentini, R., and Vesala, T.: 2000, 'Estimates of the Annual Net Carbon and Water Exchange of Forests: The EUROFLUX Methodology', *Adv. Ecol. Res.* **30**, 113–175.

Baldocchi, D.: 1994, 'A Comparative Study of Mass and Energy Exchange Rates over a Closed C3 (Wheat) and an Open C4 (Corn) Crop: II. CO_2 Exchange and Water Use Efficiency', *Agric. For. Meteorol.* **67**, 291–321.

Baldocchi, D., Falge, E., and others: 2001, 'FLUXNET: A New Tool to Study Ecosystem Metabolism and Hydrology', *Bull. Amer. Meteorol. Soc.* **82**, 2415–2434.

Baldocchi, D., Finnigan, J., Wilson, K., Paw U, K. T., and Falge, E.: 2000, 'On Measuring Net Ecosystem Carbon Exchange over Tall Vegetation on Complex Terrain', *Boundary-Layer Meteorol.* **96**, 257–291.

Black, T. A., den Hartog, G., Neumann, H. H., Blanken, P. D., Yang, P. C., Russell, C., Nesic, Z., Lee, X., Chen, S. G., Staebler, R., and Novak, M. D.: 1996, 'Annual Cycles of Water Vapour and Carbon Dioxide in and above a Boreal Aspen Forest', *Global Change Biol.* **2**, 219–229.

Blanken, P. D., Black, T. A., Yang, P. C., Neumann, H. H., Nesic, Z., Staebler, R., den Hartog, G., Novak, M. D., and Lee, X.: 1997, 'Energy Balance and Canopy Conductance of a Boreal Aspen Forest: Partitioning Overstory and Understory Components', *J. Geophys. Res.* **102**, 28915–28927.

Camp, D. W. and Kaufman, J. W.: 1970, 'Comparison of Tower Influence on Wind Velocity for NASA's 150-Meter Meteorological Tower and a Wind Tunnel Model of the Tower', *J. Geophys. Res.* **75**, 1117–1121.

Cermak, J. E. and Horn, J. D.: 1968, 'Tower Shadow Effect', *J. Geophys. Res.* **73**, 1869–1876.

Dabberdt, W. F.: 1968, 'Tower-Induced Errors in Wind Profile Measurements', *J. Appl. Meteorol.* **7**, 359–366.

Finnigan, J.: 1999, 'A Comment on the Paper by Lee (1998): "On Micrometeorological Observations of Surface-Air Exchange over Tall Vegetation" ', *Agric. For. Meteorol.* **97**, 55–64.

Finnigan, J. and Brunet, Y.: 1995, 'Turbulent Airflow in Forests on Flat and Hilly Terrain', in M. P. Coutts and J. Grace (eds.), *Wind and Trees*, Cambridge University Press, pp. 3–40.

Garratt, J. R.: 1990, 'The Internal Boundary Layer – A Review', *Boundary-Layer Meteorol.* **50**, 171–203.

Garratt, J. R.: 1992, *The Atmospheric Boundary Layer*, Cambridge University Press, New York, 316 pp.

Goulden, M. L., Daube, B. C., Fan, S. M., Sutton, D. J., Bazzaz, A., Munger, J. W., and Wofsy, S. C.: 1997 'Physiological Responses of a Black Spruce Forest to Weather', *J. Geophys. Res.* **102**, 28987–28996.

Hollinger, D. Y, Goltz, S. M., Davidson, E. A., Lee, J. T., Tu, K., and Valentine, H. T.: 1999, 'Seasonal Patterns And Environmental Control of Carbon Dioxide and Water Vapour Exchange in an Ecotonal Boreal Forest', *Global Change Biol.* **5**, 891–902.

Hollinger, D. Y., Kelliher, F. M., Byers, J. N., Hunt, J. E., McSeveny, T. M., and Weir, P. L.: 1994, 'Carbon Dioxide Exchange between an Undisturbed Old-Growth Temperate Forest and the Atmosphere', *Ecology* **75**, 134–150.

Horst, T. W. and Weil, J. C.: 1992, 'Footprint Estimation for Scalar Flux Measurements in the Atmospheric Surface Layer', *Boundary-Layer Meteorol.* **59**, 279–296.

Izumi, Y. and Barad, M. L.: 1970, 'Wind Speed as Measured by Cup and Sonic Anemometers and Influenced by Tower Structure', *J. Appl. Meteorol.* **9**, 851–856.

Kelliher, F. M., Leuning, R., Raupach, M. R., and Schulze, E.-D.: 1995, 'Maximum Conductances for Evaporation from Global Vegetation Types', *Agric. For. Meteorol.* **73**, 1–16.

Lang, A. R. G., Evans, G. N., and Ho, P. Y.: 1974, 'The Influence of Local Advection on Evapotranspiration from Irrigated Rice in a Semi-Arid Region', *Agric. For. Meteorol.* **13**, 5–13.

Lee, X.: 1998, 'On Micrometeorological Observations of Surface-Air Exchange over Tall Vegetation', *Agric. For. Meteorol.* **91**, 39–49.

Lee, X. and Black, T. A.: 1993, 'Atmospheric Turbulence within and above a Douglas-Fir Stand. Part II: Eddy Fluxes of Sensible Heat and Water Vapour', *Boundary-Layer Meteorol.* **64**, 369–389.

Lee, X., Bullock Jr., O. R., and Andres, R. J.: 2001, 'Anthropogenic Emission of Mercury to the Atmosphere in the Northeast United States', *Geophys. Res. Lett.* **28**, 1231–1234.

Lee, X., Fuentes, J. D., Staebler, R. M., and Neumann, H. H.: 1999, 'Long-Term Observation of the Atmospheric Exchange of CO_2 with a Temperate Deciduous Forest in Southern Ontario, Canada', *J. Geophys. Res.* **104**, 15975–15984.

McMillen, R. T.: 1988, 'An Eddy-Correlation Technique with Extended Applicability to Non-Simple Terrain', *Boundary-Layer Meteorol.* **43**, 231–245.

Miller, D. O., Tong, C., and Wyngaard, J. C.: 1999, 'The Effects of Probe-Induced Flow Distortion on Velocity Covariances: Field Observations', *Boundary-Layer Meteorol.* **91**, 483–493.

Moses, H. and Daubek, H. G.: 1961, 'Errors in Wind Measurements Associated with Tower-Mounted Anemometers', *Bull. Amer. Meteorol. Soc.* **42**, 190–194.

Paw U, K. T., Baldocchi, D. D., Meyers, T. P., and Wilson, K. B.: 2000, 'Correction of Eddy-Covariance Measurements Incorporating Both Advective Effects and Density Fluxes', *Boundary-Layer Meteorol.* **97**, 487–511.

Philip, J. R.: 1959, 'The Theory of Local Advection: I', *J. Meteorol.* **16**, 535–547.

Press, W. H., Teukolsky, S. A., Vetterling, W. T., and Flannery, B. P.: 1992, *Numerical Recipes in Fortran*, 2nd Edition, Cambridge University Press, 963 pp.

Rider, N. E., Philip, J. R., and Bradley, E. F.: 1963, 'The Horizontal Transport of Heat and Moisture – A Micrometeorological Study', *Quart. J. Roy. Meteorol. Soc.* **89**, 507–531.

Rochette, P., Desjardins, R. D., Pattey, E., and Lessard, R.: 1995, 'Crop Net Carbon Dioxide Exchange Rate and Radiation Use Efficiency in Soybean', *Agron. J.* **87**, 22–28.

Schmid, H. P.: 1994, 'Source Areas for Scalars and Scalar Fluxes', *Boundary-Layer Meteorol.* **67**, 293–318.

Schmid, H. P., Grimmond, C. S. B., Cropley, F., Offerle, B., and Su, H. B.: 2000, 'Measurements of CO_2 and Energy Fluxes over a Mixed Hardwood Forest in the Mid-Western United States', *Agric. For. Meteorol.* **103**, 357–374.

Spittlehouse, D. L.: 1989, 'Estimating Evapotranspiration from Land Surfaces in British Columbia', in T. A. Black, D. L. Spittlehouse, M. D. Novak, and T. D. Price (eds.), *Estimation of Areal Evapotranspiration*, IAHS Publication No. 177, pp. 245–256.

Taylor, P. A., Mason, P. J., and Bradley, E. F.: 1987, 'Boundary-Layer Flow over Low Hills', *Boundary-Layer Meteorol.* **39**, 107–132,

Tennekes, H. and Lumley, J. L.: 1972, *A First Course in Turbulence*, The MIT Press, 300 pp.

Valentini, R., Matteucci, G., Dolman, A. J., Schulze E. D., Rebmann, C., Moors, E. J., Granier, A., Gross, P., Jensen, N. O., Pilegaard, K., Lindroth, A., Grelle, A., Bernhofer, C., Grunwald, T., Aubinet, M., Ceulemans, R., Kowalski, A. S., Vesala, T., Rannik, Ü., Berbigier, P., Loustau, D., Guomundsson, J., Thorgeirsson, H., Ibrom, A., Morgenstern, K., Clement, R., Moncrieff, J., Montagnani, L., Minerbi, S., and Jarvis, P. G.: 2000, 'Respiration as the Main Determinant of Carbon Balance in European Forests', *Nature* **404**, 861–865.

Verma, S. B., Baldocchi, D. D., Anderson, D. E., Matt, D. R., and Clement, R. J.: 1986, 'Eddy Fluxes of CO_2, Water Vapor, and Sensible Heat over a Deciduous Forest', *Boundary-Layer Meteorol.* **36**, 71–91.

Wilson, K. B. and Baldocchi, D. D.: 2000, 'Seasonal and Interannual Variability of Energy Fluxes over a Broadleaved Temperate Deciduous Forest in North America', *Agric. For. Meteorol.* **100**, 1–18.

Winer, H. I.: 1955, *History of the Great Mountain Forest, Litchfield County, Connecituct*, Ph.D. Thesis, Yale University, 305 pp.

Wofsy, S. C., Goulden, M. L., Munger, J. W., Fan, S.-M., Bakwin, P. S., Daube, B. C., Bassow, S. L., and Bazzaz, F. A.: 1993, 'Net Exchange of CO_2 in a Mid-Latitude Forest', *Science* **260**, 1314–1317.

Yi, C., Davis, K. J., Bakwin, P. S,, Berger, B. W., and Marr, L. C.: 2000, 'Influence of Advection on Measurements of the Net Ecosystem-Atmosphere Exchange of CO_2 from a Very Tall Tower', *J. Geophys. Res.* **105**, 9991–9999.